

Topical Delivery of Anti-VEGF Drugs to the Ocular Posterior Segment Using Cell-Penetrating Peptides

Felicity de Cogan,¹ Lisa J. Hill,¹ Aisling Lynch,² Peter J. Morgan-Warren,¹ Judith Lechner,² Matthew R. Berwick,³ Anna F. A. Peacock,³ Mei Chen,² Robert A. H. Scott,⁴ Heping Xu,² and Ann Logan¹

¹Institute of Inflammation and Ageing, University of Birmingham, Birmingham, United Kingdom

²Centre for Experimental Medicine, Queen's University Belfast, Belfast, United Kingdom

³School of Chemistry, University of Birmingham, Birmingham, United Kingdom

⁴Moorfields Eye Hospital Dubai, Dubai, United Arab Emirates

Correspondence: Felicity de Cogan, Institute of Inflammation and Ageing, College of Medical and Dental Sciences, Vincent Drive, University of Birmingham, Birmingham, B15 2TT, United Kingdom; f.decogan@bham.ac.uk.

FdC and LJH contributed equally to the work presented here and should therefore be regarded as equivalent authors.

Submitted: June 6, 2016
Accepted: March 26, 2017

Citation: de Cogan F, Hill LJ, Lynch A, et al. Topical delivery of anti-VEGF drugs to the ocular posterior segment using cell-penetrating peptides. *Invest Ophthalmol Vis Sci.* 2017;58:2578-2590. DOI:10.1167/iovs.16-20072

PURPOSE. To evaluate the efficacy of anti-VEGF agents for treating choroidal neovascularization (CNV) when delivered topically using novel cell-penetrating peptides (CPPs) compared with delivery by intravitreal (ivit) injection.

METHODS. CPP toxicity was investigated in cell cultures. Ivit concentrations of ranibizumab and bevacizumab after topical administration were measured using ELISA. The biological efficacy of topical anti-VEGF + CPP complexes was compared with ivit anti-VEGF injections using an established model of CNV.

RESULTS. CPPs were nontoxic in vitro. In vivo, after topical eye drop delivery, CPPs were present in the rat anterior chamber within 6 minutes. A single application of CPP + bevacizumab eye drop delivered clinically relevant concentrations of bevacizumab to the posterior chamber of the rat eye in vivo. Similarly, clinically relevant levels of CPP + ranibizumab and CPP + bevacizumab were detected in the porcine vitreous and retina ex vivo. In an established model of CNV, mice treated with either a single ivit injection of anti-VEGF, twice daily CPP + anti-VEGF eye drops or daily dexamethasone gavage for 10 days all had significantly reduced areas of CNV when compared with lasered eyes without treatment.

CONCLUSIONS. CPPs are nontoxic to ocular cells and can be used to deliver therapeutically relevant doses of ranibizumab and bevacizumab by eye drop to the posterior segment of mouse, rat, and pig eyes. The CPP + anti-VEGF drug complexes were cleared from the retina within 24 hours, suggesting a daily eye drop dosing regimen. Daily, topically delivered anti-VEGF with CPP was as efficacious as a single ivit injection of anti-VEGF in reducing areas of CNV in vivo.

Keywords: ocular drug delivery, cell-penetrating peptides, delivery of ranibizumab

In neovascular AMD (nAMD), VEGF stimulates growth of blood vessels from the choroidal vasculature through damaged Bruch's membrane and into the retina. This leads to compromised retinal function and ultimately retinal damage, a condition for which anti-VEGF treatments are well established.^{1,2} To attenuate the progressive visual loss, anti-VEGF drugs are injected directly into the posterior segment of the eye, which arrests the dysregulated vascularization process.³ Although anti-VEGF drugs are extremely successful treatments for these vascular diseases, their repeated delivery by intravitreal (ivit) injection is very stressful to patients, costly to administer, and associated with significant complications, including retinal detachment, subconjunctival hemorrhage, uveitis, and endophthalmitis,^{3,4} all of which lead to poor patient compliance.³ Therefore, there is an urgent and unmet need for an alternative and less invasive drug-delivery route.^{5,6}

Cell-penetrating peptides (CPPs) have been investigated as a potential method of drug delivery since the discovery of the protein transduction domain in the HIV-1 tat peptide in 1988.⁷⁻⁹ The internalization mechanism of these transduction peptide-containing proteins into cells has not been fully

elucidated, with conflicting evidence for both active and passive processes.¹⁰⁻¹³ Although short-sequence peptides have been effectively used as chaperone agents to enhance the delivery of small molecule therapeutics to retina cells following subretinal injection,¹⁴ there is little evidence demonstrating their utility as chaperones for large drug molecules aiding their delivery to posterior segment tissues following topical application to the cornea. Once proven, this route of drug delivery would provide an alternative to the ivit injections used in nAMD clinics.

Delivery of large and small drug molecules into the eye by topical administration is a major challenge due to the unique anatomy and physiology of the eye.¹⁵ The various layers of the cornea, conjunctiva, sclera, and retina, along with the vascular blood-aqueous and blood-retinal barriers, create formidable static obstacles to drug penetration.¹⁶ Dynamic impediments to drug delivery include the choroidal and conjunctival blood flow, lymphatic clearance, efflux pumps, and tear dilution.¹⁷ These barriers combine to resist ocular drug delivery, especially to tissues in the posterior segment. Virtually all currently used eye drop formulations deliver their active agent (usually a small



molecule drug) through the cornea, sclera, and conjunctiva tissues by passive diffusion down the concentration gradient, thereby accessing the anterior segment, with a small minority of drugs also reaching the posterior segment in therapeutically relevant concentrations.^{18,19}

The therapeutic half-life of a drug is determined by its potency, local titers, and bioavailability. Once inside the eye, drugs are eliminated anteriorly via the aqueous outflow portals or posteriorly through permeation of the blood-retinal barrier.²⁰ Retinal delivery of clinically relevant quantities of large drugs, like antibodies, by repeated topical administration to the cornea has not yet been achieved. Large, negatively charged biopharmaceutical macromolecules, such as ranibizumab (Lucentis; Pharmaceuticals UK, Camberley, UK) (48 kD) and bevacizumab (Avastin; Genentech, San Francisco, CA, USA) (149 kD), are administered as repeated ivit injections to access retinal tissues.^{1,21} However, drug administration through this route is invasive and carries the risk of significant complications, giving a relatively high cost-to-benefit ratio.²²

Oligoarginine CPPs of varying lengths have previously been used to aid drug delivery. For example, protein-peptide complexes have been formed from intermolecular interactions between oligoarginine and insulin proteins. These complexes have cell-penetrating properties and are bioactive so that, for example, peptides such as HWSYILRPRRRRRRK deliver functional insulin across the gut epithelium both in vitro and in vivo.²³ Similarly, oligoarginine CPPs (RRRRRRR), covalently linked to the topical anti-inflammatory drug cyclosporine A, have enhanced drug penetration of the stratum cornea of the skin to access the underlying epidermis.²⁴

The aim of this study was to assess the potential for CPPs as chaperones within a topical ocular drug-delivery platform for the passage of therapeutic titers of high molecular weight VEGF antagonists to the posterior segment of the eye. Utilization of novel CPPs as ocular drug-delivery agents would facilitate clinical administration of large biopharmaceuticals, such as ranibizumab or bevacizumab, in the form of an eye drop. The development of this eye drop delivery platform will have wide-reaching implications for improved patient care, by reducing the side effects and treatment costs associated with both current clinically effective drugs and novel candidate drugs. Here, we have evaluated CPP-mediated eye drop delivery of anti-VEGF antibodies in rodent and porcine models to determine dose delivery and pharmacokinetics. We also have used an established in vivo rodent model of choroidal neovascularization (CNV) to compare the efficacy of anti-VEGF drugs when delivered topically with CPPs or by intravitreal injection.

MATERIALS AND METHODS

Animal Experiments

All animal procedures were performed under license in accordance with the UK Home Office Animals Scientific Procedures Act 1986 and the ARVO Statement for the Use of Animals in Ophthalmic and Vision Research.

Synthesis of CPPs

CPP (5[6]-carboxyfluorescein-RRRRRR-COOH) synthesis was performed on a 1-mmol scale on preloaded Fmoc-Nw-(2,2,4,6,7-pentamethylidihydrobenzofuran-5-sulfonyl)-L-arginine Wang resin (Sigma-Aldrich, Poole, UK) (loading rate 0.62 mmol g⁻¹) using standard Fmoc-amino acid solid-state peptide synthesis protocols. The initial Fmoc group was removed by deprotection with 20% piperidine in *N,N*-dimethylformamide

(DMF) (3 × 20 minutes), followed by coupling with Fmoc-Nw-(2,2,4,6,7-pentamethylidihydrobenzofuran-5-sulfonyl)-L-arginine in the presence of *O*-(6-chlorobenzotriazol-1-yl)-*N,N,N',N'*-tetramethyluronium hexafluorophosphate (HCTU), *N,N*-diisopropylethylamine (DIPEA), and DMF in a 1:5:5:10 molar ratio. The reaction was agitated at room temperature for 8 hours, and some of the resin was tested for reaction completion using the ninhydrin test following standard protocols.²⁵ The coupling and deprotection steps were repeated until the peptide sequence reached a total of six arginine residues. The final Fmoc group was removed, the resin washed with DMF and dichloromethane (DCM), and the free N-terminus was coupled with 5(6)-carboxyfluorescein in the presence of HCTU and DIPEA in a 1:5:5:10 molar ratio in DMF for 8 hours, to give an inbuilt fluorescent tag. After washes with DMF, DCM, and diethyl ether, the resin was air dried for 1 hour. The peptide was cleaved from the resin using trifluoroacetic acid (TFA) (27 mL), thioanisole (1.5 mL), 1,2-ethanedithiol (0.9 mL), and anisole (0.6 mL) under N₂ with agitation in the dark for 3 hours, with simultaneous removal of side-chain protecting groups. Resin was removed by filtration and the crude peptide precipitated out of solution in cold diethyl ether and storage at -20°C for 8 hours. The precipitate was isolated by centrifugation at 2164g for 10 minutes and removal of the diethyl ether. The peptide was purified by preparative reversed-phase HPLC on a Phenomenex Luna C12 column (250 × 21.2 C12 [2] 10-μm Jupiter Proteo 90-Å Axia Packed [Phenomenex, Macclesfield, UK]) with a solvent mixture altered with a linear gradient from 0.1% TFA in water to 0.1% TFA in CH₃CN over 40 minutes. The isolated peptide was lyophilized to yield a yellow solid (258 mg, 19.6% yield at 97% purity), which was identified by electrospray ionization mass spectrometry. Stock solutions of the peptide were prepared in sterile PBS and stored at 4°C until use.

CPP-Therapeutic Complex Formation

CPPs (5 mg) were dissolved in stock solutions of bevacizumab (25 mg/mL; Roche Pharmaceuticals, Welwyn Garden City, UK) or ranibizumab (10 mg/mL; Novartis Pharmaceuticals UK). The solution was vortexed for 10 seconds and stored at 4°C until use.

Circular Dichroism Analysis of CPP + Drug Complexes

Circular dichroism (CD) was used to characterize the effect of concentration on CPP + bevacizumab complex formation. CD spectra were recorded in 1-mm pathlength quartz cuvettes on a Jasco J-715 spectropolarimeter (Jasco UK, Great Dunmow, UK).²⁶ The stock solution of bevacizumab (125 μg/mL) was read at 200 to 300 nm. A stock solution of CPP was prepared at 1000 μg and diluted into the bevacizumab solution. The observed ellipticity was converted to molar ellipticity.

In Vitro Cytotoxicity Assays

Primary Adult Rat Retinal Cell Cultures. Adult rats (Sprague-Dawley; Charles River, Kent, UK) were killed by CO₂ overdose and their eyes removed and the neural retinae dissociated into single cells by using a papain dissociation kit, in accordance with the manufacturer's instructions (Worthington Biochemicals, Lakewood, NJ, USA). Mixed retinal cells, containing retinal ganglion cells (RGCs), were seeded at a density of 125,000 cells/well in 8-well chamber slides (BD Biosciences, Erembodegem, Belgium), precoated with poly-D-lysine and laminin (20 μg/mL) in 300-μL/well Neurobasal-A supplemented with B27 supplement and gentamicin (all from

Invitrogen, Paisley, UK).²⁷ Retinal cell cultures were incubated overnight at 37°C and 5% CO₂ and were treated the following day with CPPs prepared from lyophilized stocks that were made up in sterile PBS (1 mg, 6.9 µM) and diluted to final concentrations of 100 µg/mL, 10 µg/mL, 1 µg/mL, and 0.1 µg/mL in 500 µL culture medium/well. After 3 days of incubation at 37°C and 5% CO₂, culture medium was removed and the cells were fixed with 4% paraformaldehyde (PFA; Taab, Reading, UK) for 10 minutes before being processed for immunocytochemistry. Retinal cells were washed with rinsing buffer (0.1% Triton-X 100 in PBS) for 3 × 5 minutes and blocking buffer (10% normal goat serum [Vector Laboratories, Peterborough, UK] and 3% BSA in rinsing buffer) was added at 150 µL/well for 30 minutes to block nonspecific protein binding. Primary antibody against the RGC phenotypic marker βIII-tubulin was added (1:200 dilution in blocking buffer, 150 µL/well) and incubated for 1 hour at room temperature. The primary antibody solution was removed; the cells were washed 3 × 5 minutes and then incubated with secondary antibody (Alexa 488 anti-mouse IgG, 1:400 dilution in blocking buffer; Invitrogen) at 150 µL/well for 1 hour in the dark. After further washes as described, the chamber wells were removed and the slides were mounted with Vectashield with 2-(4-amidinophenyl)-6-indolecarbamide dihydrochloride (DAPI) (Vector Laboratories). The stained slides were viewed with an Axioplan-2 fluorescence microscope and images were obtained with Axiovision software (both Carl Zeiss, Ltd., Hertfordshire, UK). Each well was divided into a grid of nine squares and two photomicrographs were taken within each square (total 18 images/well). Surviving βIII-tubulin⁺ RGCs were counted from these images and cell numbers per well determined from two wells per condition in three independent biological replicates.

Adult Human RPE (ARPE-19) Cell Cultures. Stock human ARPE-19 cells²⁸ (CRL-2032; ATCC, Middlesex, UK) were cultured in T75 flasks (Sarstedt, Leicester, UK) in Dulbecco's modified Eagle's medium with fetal bovine serum (10%, vol/vol) (both from Life Technologies, Paisley, UK). The cells were passaged at 70% confluency by the addition of trypsin-EDTA (2.5 mL) with a 5-minute incubation at 37°C, followed by replating. Cells were used between passage 4 and passage 10. Cells for experiments were seeded into 24-well cell culture plates (Fisher Scientific, Loughborough, UK) at a cell density of 25,000 cells per well. A CPP solution was made from lyophilized stock in sterile PBS (1 mg, 6.9 µM) and diluted to 100 µg/mL, 10 µg/mL, 1 µg/mL, 0.1 µg/mL in the cell culture media. The ARPE-19 cells were incubated at 37°C for 3 days, after which the media was removed and the cell monolayer washed with PBS (1 mL). Fresh media (1 mL) was added to each well with alamar blue salt (Sigma-Aldrich) diluted in sterile PBS (10 µL, 150 µM).²⁹ Wells with no cells present were run as a technical control. The cells were incubated for 2 hours at 37°C for the alamar blue to be metabolized, after which the alamar blue-containing media was transferred to wells in a 96-well plate and the absorbance read at 570 nm (λ_{max} alamar blue) using a Glomax multi-detection system (Promega, Southampton, UK). Cell number was calculated by comparing the measured absorbance against a standard curve of absorbance against known cell number.³⁰

Primary Adult Human Corneal Fibroblast Cultures.

Primary human corneal fibroblast (hCF) cells were cultured in T75 flasks (Sarstedt) RPMI 1640 media supplemented with fetal bovine serum (10% vol/vol) and 1% penicillin/streptomycin (Invitrogen). Stock cell cultures were passaged at 70% confluency using trypsin-EDTA. Experimental cells were seeded in the same medium into 24-well cell culture plates (Fisher Scientific) at a cell density of 50,000 cells per well. A

CPP solution was prepared as described previously in sterile PBS (1 mg, 6.9 µM) and diluted to 100 µg/mL, 10 µg/mL, 1 µg/mL, and 0.1 µg/mL in the cell culture media and the cells were incubated with the various concentrations at 37°C for 3 days. The medium was removed and the hCF monolayers washed three times by the addition and removal of PBS (1 mL). Fresh media (1 mL) was added to each well together with alamar blue salt in sterile PBS (10 µL, 150 µM). The cells were incubated for 2 hours at 37°C for the alamar blue to be metabolized, after which the alamar blue-containing media was transferred to wells in a 96-well plate and the absorbance read on a Glomax multidetection system at 570 nm (λ_{max} alamar blue). Control samples containing media and alamar blue without cells were also run as an assay control. hCF number was calculated by comparing with a standard curve of absorbance (measure of metabolism rate) obtained from a known range of cell number.

In Vivo Anterior Segment Imaging of CPP Passage Into the Rat Eye

Male Sprague-Dawley rats (200 g) (Charles River) were anesthetized by using 5% isoflurane (National Vet Supplies, Stoke, UK) under Home Office Licence 30/2720. The rats had a 20-µL CPP eye drop applied to the cornea and the eyes were imaged using a Spectralis Anterior Segment Module on the Heidelberg Spectralis optical coherence tomography (OCT) system (Heidelberg Engineering, Heidelberg, Germany) every 30 seconds for 10 minutes.

In Vivo CPP Delivery of Anti-VEGF Into the Vitreous of Rat Eyes and the Time Course of Anti-VEGF Clearance From the Vitreous and Retina

Under Home Office Licence 30/2720, adult male Sprague-Dawley rats (200 g) (Charles River) had a single 20-µL eye drop containing CPP (5 µg/µL), CPP (5 µg/µL) + bevacizumab (25 µg/µL), bevacizumab (25 µg/µL), or PBS applied topically to the corneal surface. The rats were rehoused and observed for well-being for 30 minutes before killing by using rising levels of CO₂ and dissection of the ocular tissues. In a second study, groups of rats were killed by rising levels of CO₂ at 20, 40, and 60 minutes plus 2, 4, and 24 hours after anti-VEGF drug delivery ($n =$ four rats per group), eyes were removed, and the vitreous and retinae were harvested together. The combined tissues were freeze-thawed and homogenized together in 110 µL sterile PBS. The level of bevacizumab in the retinal homogenate was measured by using a Protein Detection ELISA kit (KPL, Gaithersburg, MD, USA) with an anti-human antibody (309-001-003; Jackson Immuno Research Laboratory, West Grove, PA, USA). Briefly, high-affinity plates (Sigma-Aldrich) were coated with 0.1 µg/mL anti-human antibody for 1 hour and the ELISA was then carried out according to manufacturer's instructions.

Ex Vivo Anti-VEGF Drug Delivery Into Porcine Eyes

Adult porcine eyes were obtained from a local slaughterhouse, stored on ice, and used within 3 hours of animal death. The eyes were irrigated with PBS and then had a 60-µL eye drop with and without drug applied to the cornea. After 45 minutes' incubation period at room temperature, eyes were washed three times with PBS and the vitreous and retina were removed. Vitreous was freeze-thawed and homogenized, retinal tissues were freeze-thawed and homogenized in 100 µL sterile PBS, the tissues were analyzed for ranibizumab and/or bevacizumab levels by ELISA, as described previously.

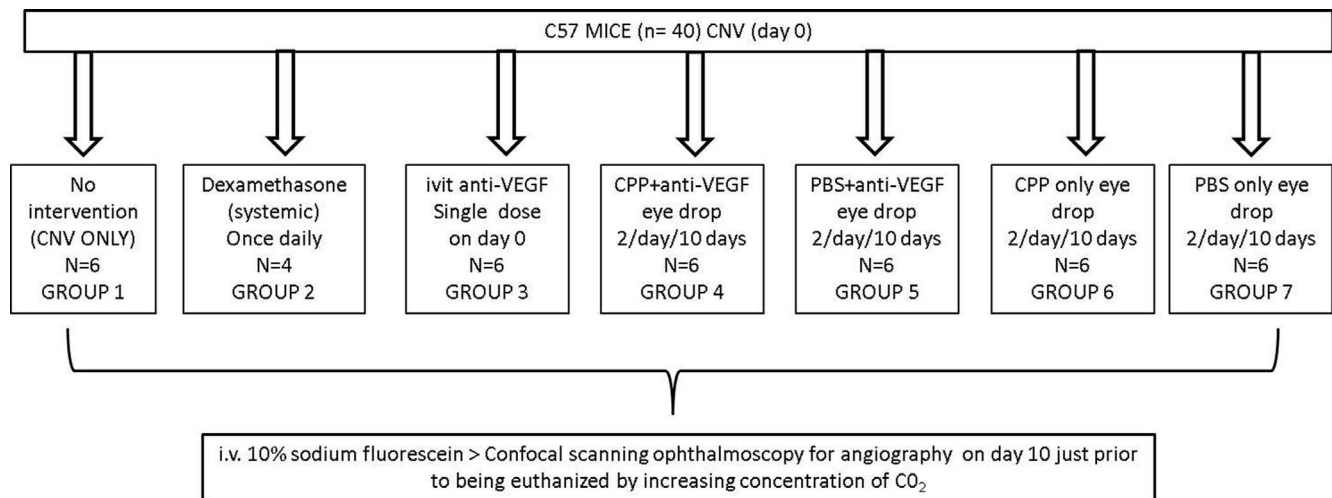


FIGURE 1. Experimental design to assess in vivo efficacy of anti-VEGF in a mouse model of CNV.

In Vivo Efficacy of Anti-VEGF Agent in a Mouse Model of CNV

Wild-type (WT) C57BL/6J mice (Harlan Laboratories, Derby, UK) were maintained within the Biological Research Unit at Queen's University Belfast and the CNV study was performed at this site in accordance with UK Home Office (Animals [Scientific Procedures] Act, 1986) guidelines and the experimental protocols were approved by the University Ethics Committee. To create CNV, mice were anesthetized by injection of Rompun (xylazine) (2% wt/vol; Bayer, Newbury, UK) and Ketaset (100 mg/mL; Fort Dodge Animal Health, Ltd., Hampshire, UK) and rupture of Bruch's membrane-choroid was achieved by laser photocoagulation (Haag Streit BM 900 Slit Lamp and Argon laser; Haag Streit, Harlow, UK) using CNV laser burns of 100- μ m spot size (0.05-second duration, 250 mW) approximately two disc-diameters away from the optic disc. Mice were randomly allocated into seven groups (Fig. 1): (1) ($n = 6$) received CNV laser burn only; (2) ($n = 4$) received CNV laser burn and treatment with 0.5 mg/kg/d for 10 days of dexamethasone delivered systemically through gavaging; (3) ($n = 6$) received CNV laser burn and treatment with a single 2- μ L intravitreal injection of 200 ng/ μ L of anti-VEGF (R&D Systems, Abingdon, UK; this is an established literature treatment of murine angiogenesis³¹⁻³⁴); (4) ($n = 6$) received CNV laser burn and treatment with a single 5- μ L eye drop containing CPP 25 μ g/5 μ L + anti-VEGF 1.8 μ g/5 μ L administered twice daily for 10 days; (5) ($n = 6$) received CNV laser burn and treatment with a single 5- μ L eye drop containing PBS + 1.8 μ g/5 μ L anti-VEGF administered twice daily for 10 days; (6) ($n = 6$) received CNV laser burn and treatment with a single 5- μ L eye drop containing CPP 25 μ g/5 μ L, only administered twice daily for 10 days; and (7) ($n = 6$) received CNV laser burn and treatment with a single 5- μ L PBS eye drop administered twice daily for 10 days. Just before killing the mice on day 10, confocal scanning laser ophthalmoscopy (Heidelberg Engineering) was carried out under anesthesia to obtain retinal angiography data immediately after intravenous injection of 100 μ L 10% sodium fluorescein.

Mice were killed by cervical dislocation and the eyes were immediately dissected and placed in 2% PFA (Sigma-Aldrich) in PBS for 2 hours. Following this, the PFA was removed and eyes were stored in PBS at 4°C for 5 days before being dissected. For dissections, the RPE/choroid/sclera was removed in its entirety and placed in PBS as a floating structure. The RPE/choroid/sclera was washed again in PBS before permeabilization in 1% Triton X-100 (Sigma-Aldrich) for 1.5 hours at room tempera-

ture. After 3 washes in PBS, the floating tissue was immersed in 1/100 primary antibody against collagen (BioRad, Hertfordshire, UK) and Isolectin B4 (Vector Laboratories) diluted in 0.5% Triton X-100 and 10% fetal calf serum (Sigma-Aldrich) in PBS and left overnight at 4°C. The following day, the tissue was washed three times in PBS, before incubation with secondary antibody (Alexa-594 for collagen and Fluorescent Strep 488 for isolectin B4; Life Technology, Warrington, UK) at dilutions of 1/200 and 1/100 in PBS + 0.2% Triton, respectively for 1.5 hours at room temperature. After washing in PBS, the tissue was flatmounted and covered with Vectashield mounting medium (Vector Laboratories).

The CNV lesion area in the flatmounted tissue was visualized with a Nikon Eclipse E400 microscope and the collagen and isolectin-positive lesion area measured to identify lesion size and new blood vessel formation and lesion size using NIS Elements (Nikon, Amsterdam, UK). All images of CNV lesions were analyzed using ImageJ (<http://imagej.nih.gov/ij/>; provided in the public domain by the National Institutes of Health, Bethesda, MD, USA). Images were assigned randomized numbers to ensure blinding of treatment groups during quantification by the assessor. The number of pixels per 100 μ m was set and used to determine area (μ m²) of the CNV lesion size shown by collagen IV and isolectin immunoreactivity. The area for each group was averaged and presented as mean \pm SEM.

Statistical Analysis

All statistical analyses were carried out using SPSS 17.0 (IBM SPSS, Inc., Chicago, IL, USA) and data were presented as mean \pm SEM. The Shapiro-Wilk test was used to ensure all data were normally distributed before parametric testing by using a 1-way ANOVA with Tukey post hoc test or a Mann-Whitney *U* test. The homogeneity of variance was analyzed for all data; where this was found to be statistically different, Games-Howell analysis was used to determine statistical significance. The statistical significance threshold was $P < 0.05$ (2-tailed).

RESULTS

CPP Forms Complexes With Bevacizumab

Complex formation was monitored using CD (Fig. 2). The 218-nm spectral peak of 0.25 mg/mL bevacizumab was -2121.5

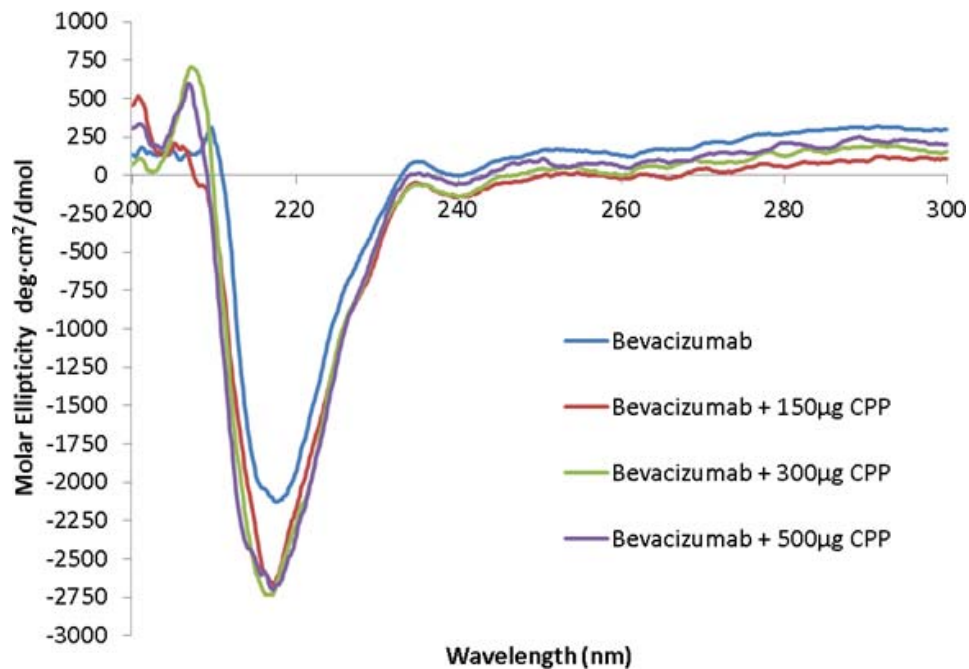


FIGURE 2. CD data of bevacizumab with increasing amounts of CPP in the electrostatic complex. This demonstrated that small amounts of CPP induce a change in the CPP + bevacizumab reflecting complex formation, but increasing the amount of the CPP does not induce further change.

deg·cm²/dmol. This peak was enhanced to -2694.9 deg·cm²/dmol when 150 µg CPP was added to bevacizumab (1 mL), to -2689.4 deg·cm²/dmol with 300 µg CPP and to 2704.7 deg·cm²/dmol with 500 µg CPP. This indicates that CPPs form a complex with bevacizumab, and that increasing the relative concentration of CPP above 150 µg does not significantly alter the complex structure.

CPPs Are Nontoxic for Rat Retinal, Human ARPE-19 Cells, and Human Corneal Fibroblasts

The CPPs were tested for cytotoxicity against a range of ocular cells before in vivo testing via continuous exposure to CPP for 3 days in culture. In primary mixed retinal cultures from adult rats, the numbers of β III-tubulin + RGC surviving after treatment with CPP at concentrations of 0.1 µg/mL, 1 µg/mL, 10 µg/mL, and 100 µg/mL were not significantly different from that in the PBS control (Fig. 3a). Similarly, in human ARPE-19 cells (Fig. 3b) cell numbers at the concentrations of 0.1 µg/mL, 1 µg/mL, 10 µg/mL, and 100 µg/mL CPP were not significantly different from that in the PBS control. There was also no effect on numbers of primary human corneal fibroblasts (Fig. 3c) surviving after 3 days of treatment with CPP at any concentration tested compared to the PBS control. These results indicate that the CPPs were not cytotoxic to ocular cells at the concentrations tested after 3 days in culture.

Eye Drop Formulations of CPP-Drug Complexes Deliver Drugs Rapidly Across the Cornea to the Anterior and Posterior Segments of the Rat Eye

Fluorescently tagged CPPs (20 µL of 5 µg/µL) were applied topically to the cornea of an anesthetized rat and OCT images were taken every 30 seconds. Fluorescent CPPs were observed in solution on the surface of the cornea at 0 minutes and were present within the anterior chamber by 6 minutes (Fig. 4A). Further eye drop studies quantified the amount of anti-VEGF antibody the CPP delivered across the cornea, to the anterior

and posterior segments, and into retinal tissue (Fig. 4B). When a 20 -µL eye drop of bevacizumab (25 µg/µL) complexed with CPP (5 µg/µL) was applied to the cornea, 1.06 ± 0.35 µg/mL of bevacizumab was detected by ELISA within tissue homogenates after 30 minutes. This represented 0.2% of the delivered payload. This level was significantly higher ($P < 0.001$) than that seen in all controls. Clearance of bevacizumab from the retina following delivery by topical application was then established by examining retinal levels of bevacizumab over time (Fig. 4C). This showed that 0.68 ± 0.26 µg/mL bevacizumab was detected within the tissue homogenates at 20 minutes after topical administration, with levels increasing to 1.65 ± 0.26 µg/mL at 40 minutes, followed by decreasing levels, with 0.4 ± 0.22 µg/mL detectable at 4 hours and 0.007 ± 0.22 µg/mL at 24 hours after topical application. This shows a clearance of bevacizumab from the rodent retina by 24 hours, suggesting a daily dosing regimen would be required to sustain therapeutic levels by eye drop drug delivery in disease model studies and also implies the need for daily dosing in humans.

CPP-Drug Complexes Access Retinal Tissues After Eye Drop Delivery to the Pig Eye

Eye drops of 20 µL, containing ranibizumab (10 µg/µL) complexed with CPP or bevacizumab (25 µg/µL) complexed with CPP, or appropriate controls, were applied topically to porcine cornea, and after 45 minutes vitreous and retinae were dissected and the levels of human IgG measured by ELISA (Figs. 5a, 5b). The levels of human IgG measured indicate that, when drugs were complexed with CPP, topical delivery achieved 17.09 ± 4.68 µg/mL of ranibizumab and of 10.68 ± 3.57 µg/mL of bevacizumab in the total vitreous. This represented significantly higher ($P < 0.001$) levels than those seen in control animals, treated with eye drops containing either uncomplexed ranibizumab, uncomplexed bevacizumab eye, CPP-alone, or PBS-alone. Similarly, 0.10 ± 0.03 µg per retina of bevacizumab was detected in the retina after application of CPP + bevacizumab complex eye drops. This was also significantly higher than levels in the control groups ($P < 0.005$).

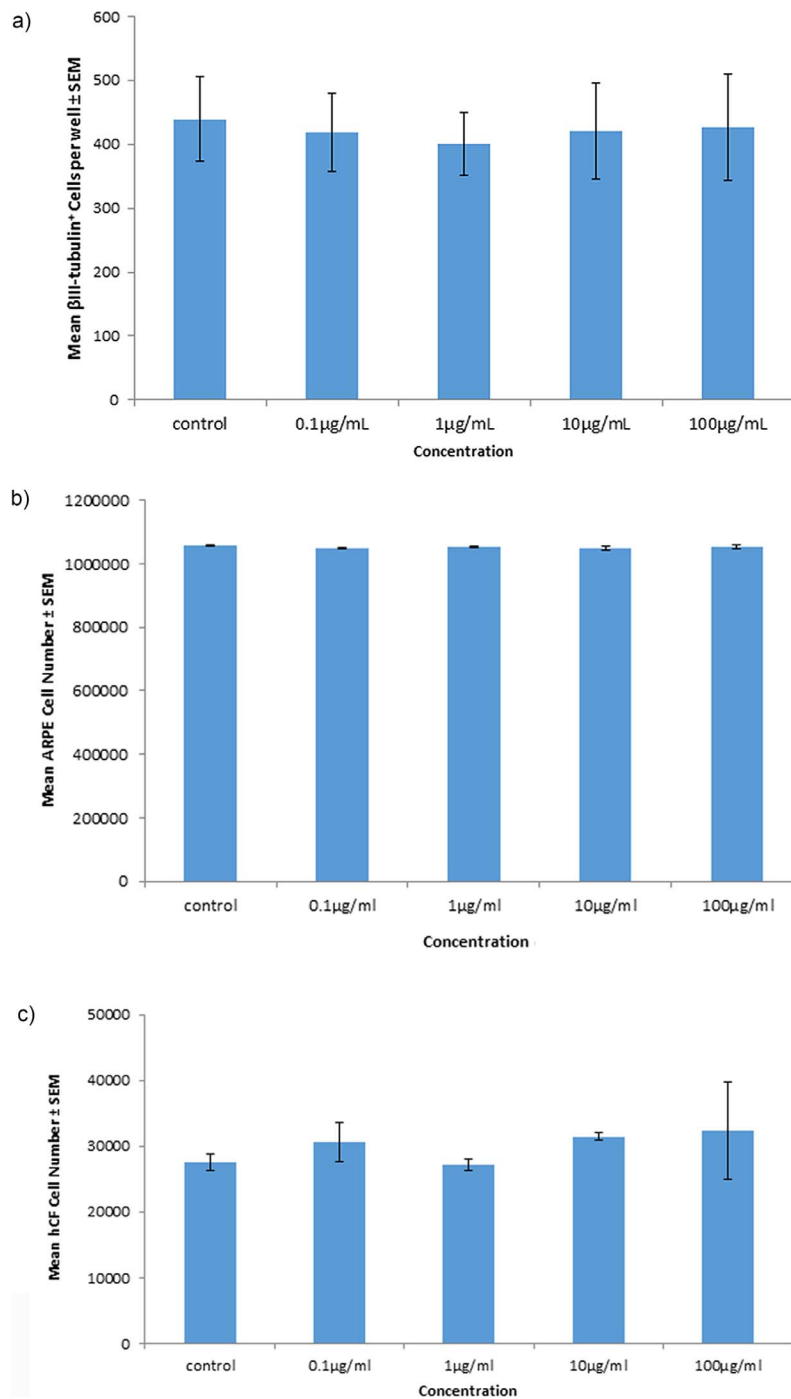


FIGURE 3. Cytotoxicity of CPP for ocular cells after 72 hours in vitro. (a) Numbers of primary rat RGC analyzed using immunocytochemistry, with values shown being averages of three biological replicates, $P > 0.05$. (b) Human ARPE cells analyzed using alamar blue assay, with values shown representing averages of three biological replicates, $P > 0.05$. (c) Primary hCF cells analyzed using alamar blue assay, with values shown being averages of three biological replicates, $P > 0.05$.

Eye Drop CPP–Anti-VEGF Complexes Attenuate Neovascularization in a Mouse Model of CNV

The bioefficacy of anti-VEGF when delivered topically complexed to CPP was determined in a mouse model of CNV. Fluorescein angiography (FA) and infrared imaging (IR) at 10 days in all groups demonstrated that eye drop delivery of CPP + anti-VEGF complexes considerably reduced the size of the laser-induced CNV lesion, characterized by an area of hyperfluorescence surrounding a core of hypofluorescence

(Fig. 6). This lesion denotes an area of high neovascularization that leads to fluorescein leakage and, therefore, the increased fluorescence levels observed. When the size of the untreated CNV fluorescent halos were compared with those in the lasered treatment group receiving eye drops containing uncomplexed anti-VEGF or the three negative control groups, no differences were apparent. By contrast, smaller CNV fluorescent halos were measured in the two positive control groups receiving daily systemic dexamethasone by gavage or a single anti-VEGF ivit injection. RPE/choroidal flatmount

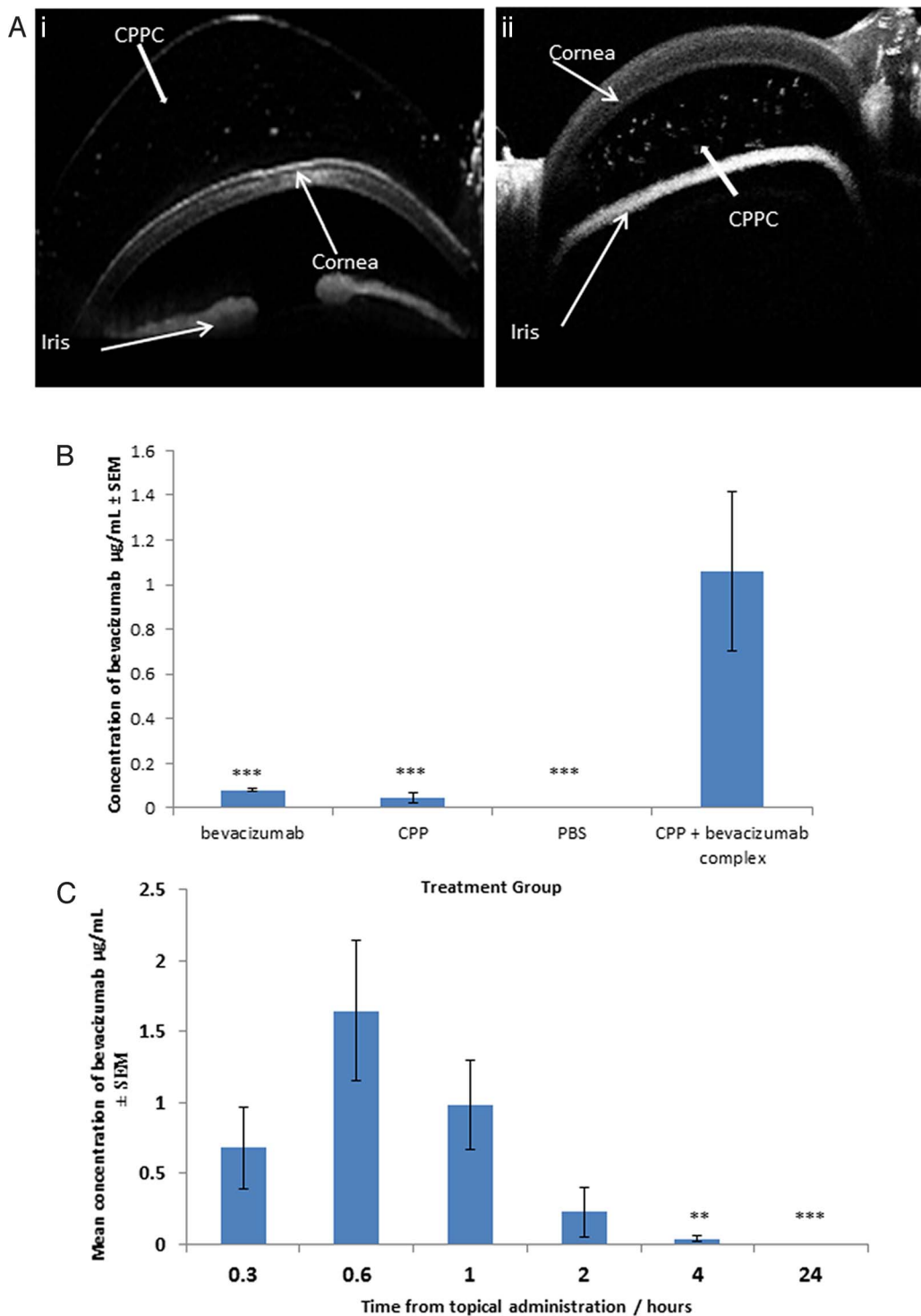


FIGURE 4. Delivery of bevacizumab to the rodent eye. (A) OCT images of fluorescent CPP entry into the anterior chamber of the eye. Fluorescently labeled CPPs were seen in a CPP eye drop on the corneal surface at $t=0$ (i) and within the anterior chamber by 6 minutes (ii). (B) ELISA data at 30 minutes demonstrates significant drug titers in the posterior segment (comprising vitreous and retina) after a single CPP + bevacizumab eye drop treatment ($n=3$; $***P < 0.01$) all groups compared with PBS control. (C) Concentrations of bevacizumab accumulating in the posterior segment (comprising vitreous and retina) over 24 hours after a single CPP + bevacizumab eye drop application ($n=4$, $**P < 0.01$, $***P < 0.001$).

immunohistochemistry of collagen IV and isolectin B4 (as markers of extracellular matrix and endothelial cells, respectively) allowed the areas of scar and neovascularization to be measured and compared (Fig. 7). This showed that the animals with CNV without further treatment showed a lesion area of collagen IV and isolectin staining of $176,195 \pm 43,396 \mu\text{m}^2$.

Lesion areas were reduced to $49,898 \pm 10,207 \mu\text{m}^2$ in animals that received daily gavage steroid treatment. A reduction to $49,817 \pm 11,015 \mu\text{m}^2$ was also seen in eyes receiving a single intravitreal anti-VEGF injection. When anti-VEGF was delivered topically complexed to CPP, a similar reduction in lesion area was observed to $48,388 \pm 5521 \mu\text{m}^2$. The lesion sizes in

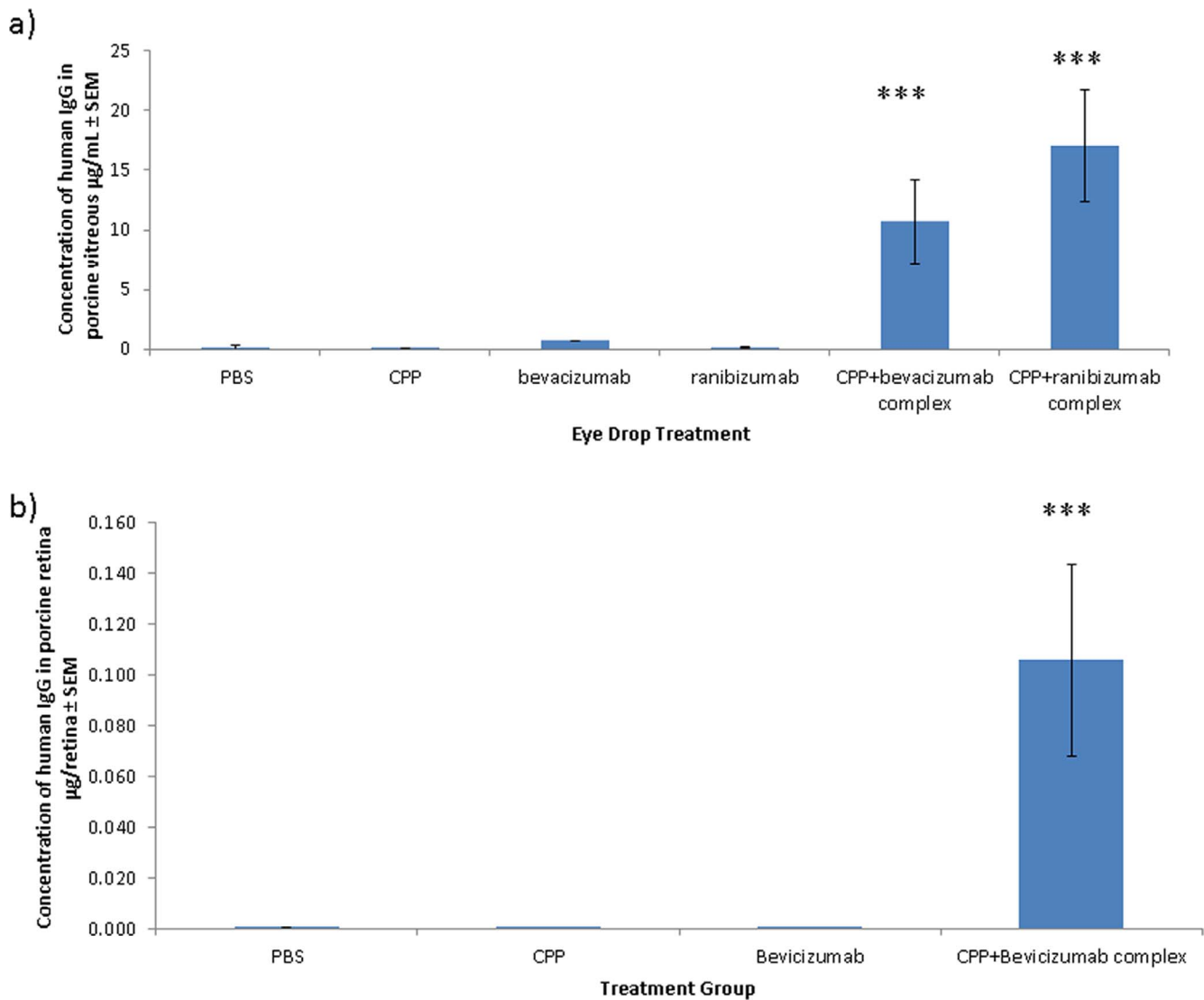


FIGURE 5. (a) Titers of bevacizumab and ranibizumab delivered to the porcine vitreous using CPP eye drops. ELISA data showed that administering CPP + anti-VEGF eye drops resulted in significantly higher microgram titers of bevacizumab and ranibizumab measured in the vitreous compared with PBS-alone (control group), CPP-alone, bevacizumab-alone, and ranibizumab-alone eye drop application. (b) Titers of bevacizumab delivered to the porcine retina using eye drops. ELISA data demonstrated that CPP + bevacizumab complexes delivered significantly higher levels of bevacizumab compared with PBS (control group), CPP-alone, and bevacizumab-alone. This demonstrates the effectiveness of CPP to carry clinically relevant titers of both drugs to the posterior segment in an eye of comparable size to the human eye ($n = 3$, $***P < 0.01$).

all three treatment groups were significantly lower than those in CNV eyes that received no treatment ($P < 0.001$), with no significant difference among the three treatment groups. Lesion areas in the negative control groups of CPP-only eye drops ($89,540 \pm 14,706 \mu\text{m}^2$), anti-VEGF-only drops ($112,802 \pm 18,855 \mu\text{m}^2$), and PBS eye drops ($105,714 \pm 25,149 \mu\text{m}^2$) were all significantly higher than those in animals that received CPP delivered anti-VEGF ($P < 0.001$), with no significant difference between these negative controls and those animals that received no treatment. These data show that daily topical administration of the CPP complexed with anti-VEGF was as efficacious as the standard single ivit injection of anti-VEGF.

DISCUSSION

Anti-VEGF agents are a well-established treatment for nAMD^{1,2}; however, the side effects from delivery by ivit injection

represent a significant problem.^{3,4} Accordingly, this study investigated the use of CPP as a novel topical delivery vehicle for anti-VEGF agents to the posterior segment, negating the need for invasive ivit injections. This study demonstrates that CPP can successfully deliver topically applied anti-VEGF drugs into mouse, rat, and pig eyes, and showed bioactivity of the topically delivered drug in a relevant disease model that was equivalent to other AMD drug-delivery methods.³⁰

The use of CPPs as drug-penetration enhancers is well described in the literature. For example, CPPs can be covalently coupled to psoriasis drugs to enhance transdermal delivery.³⁵ Although this study further illustrates the clinical potential of penetration enhancers, CPP platform technologies have not previously been established, as each drug has been delivered using a novel CPP attachment method. For example, previous work by Johnson et al.³⁶ reports the delivery of green fluorescent protein to the cornea after topical application and to the retina after ivit injection. However, this work relied on

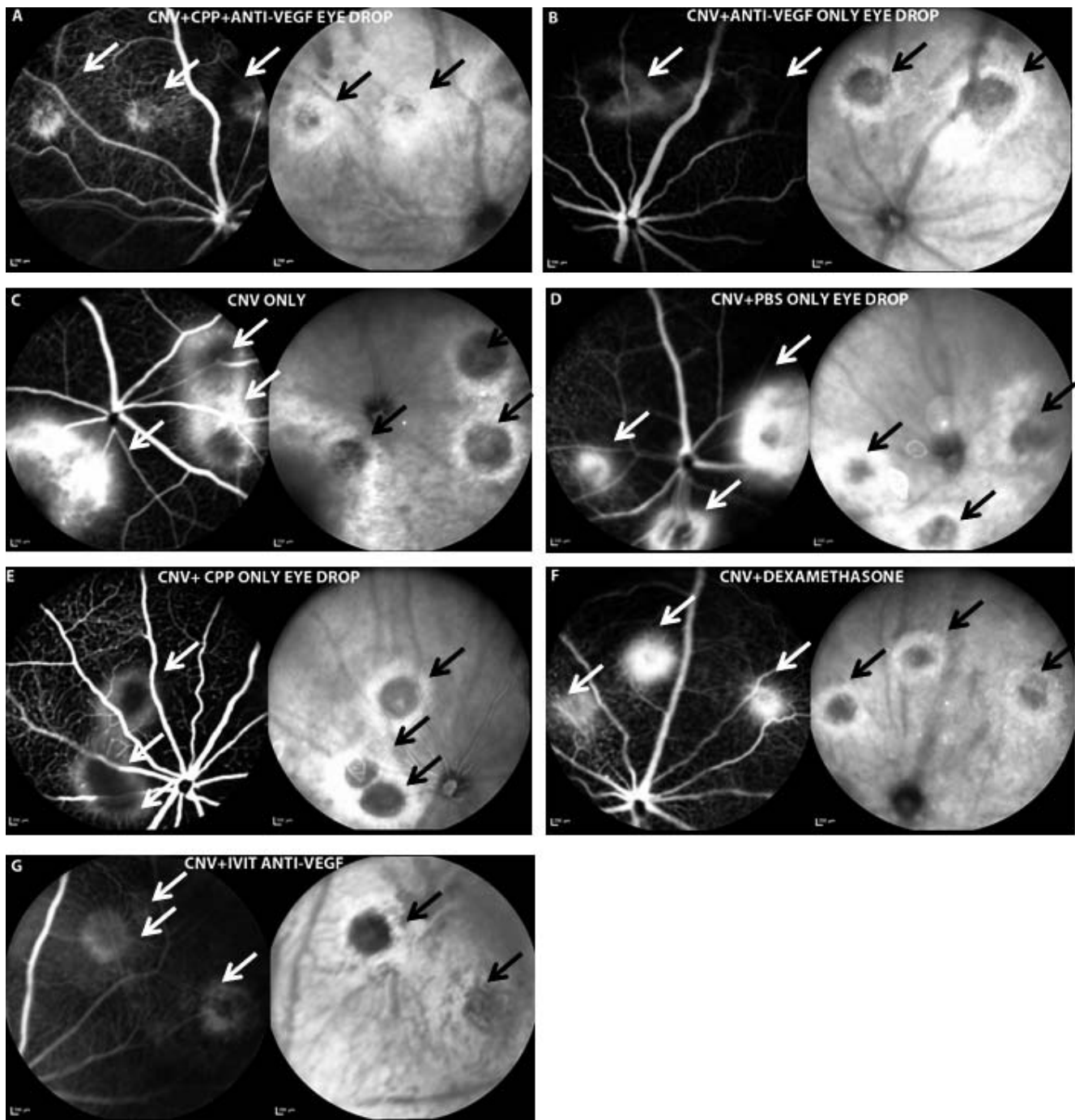


FIGURE 6. In vivo live scanning laser ophthalmoscope (SLO) images of FA (*left*) and IR (*right*) of mouse retinæ after laser induction of CNV wounds. In both FA (*black arrows*) and IR (*white arrows*) images, CNV laser lesions are apparent as halos of leaked fluorescein from retinal blood vessels, with light areas of hyperfluorescence surrounding a central dark hypo-fluorescent core (*scale bar*: 200 μ m). Using SLO to perform both FA and IR together allows the identification of potential areas of damage in both retina and choroid.

grafting the CPP to the therapeutic load and (for posterior segment delivery) an injection either intravitreally or subretinally.³²

In contrast, here we have exploited simple charge-based interactions between the CPP and the therapeutic to formulate drug complexes that are decorated by the CPP. This enhances drug passage across tissue barriers, both into cells and between cells, and also ensures that drug bioefficacy is not compromised by the permanent attachment of the CPP unit onto the drug molecule. Accordingly, current drug stockpiles and

methods of manufacture can be used in preparing the CPP-drug complexes.

The CPP concentration estimated in different anatomical compartments through the eye after eye drop delivery informed the in vitro investigations into CPP toxicity for ocular cells after 3 days in culture. Examination of the literature shows that poly-arginine-based CPPs have been tested extensively against many cell types, with reports conflicting whether CPPs inflict toxic effects on cells.³⁷⁻³⁹ Here, topical delivery by eye drop delivered 5 mg/mL CPP onto the cornea,

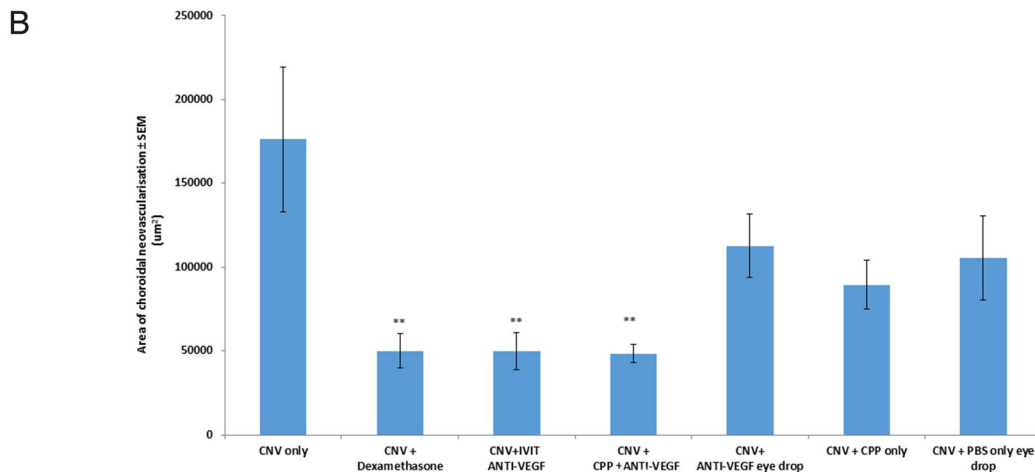
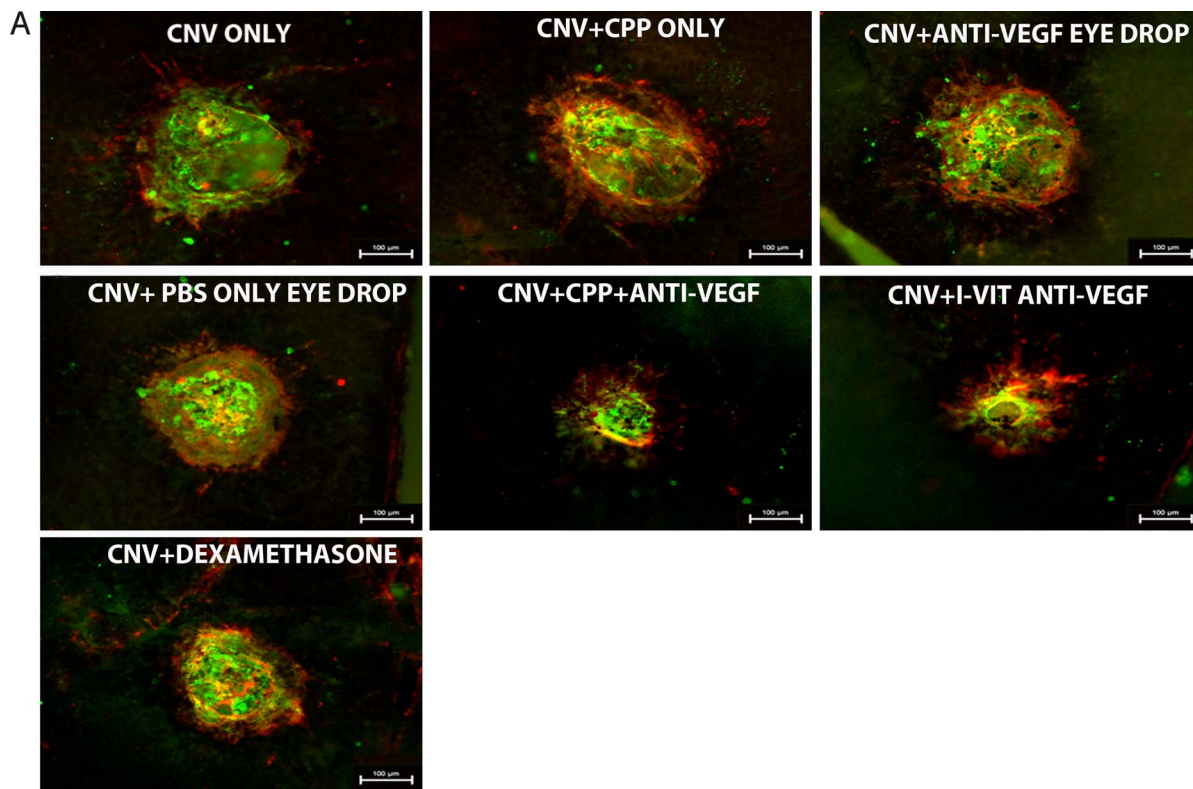


FIGURE 7. Immunohistochemical staining of retinal CNV lesions confirmed no difference between ivit anti-VEGF and CPP + anti-VEGF eye drops. **(A)** Immunohistochemical staining of the neovascularization in CNV lesions (collagen IV: red, isolectin B4: green) confirmed that, compared with untreated CNV-only retinæ, vascular lesions were smaller after treatment with CPP + anti-VEGF eye drops, ivit injection of anti-VEGF, and systemic dexamethasone. Anti-VEGF, PBS (experimental and statistical control), and unloaded CPP eye drops did not affect CNV size (scale bar: 100 μm). **(B)** Quantitation of areas of isolectin B4 + CNV lesions. Compared with untreated controls, CNV lesions in mice receiving CPP + anti-VEGF eye drops, ivit injection of anti-VEGF, and systemic dexamethasone were all similarly reduced ($n = 6$, $**P < 0.001$), whereas CNV lesion sizes were unchanged after topical treatment with anti-VEGF, PBS, and unloaded CPP eye drops.

with 85 μg/mL calculated to be present in the posterior segment after 30 minutes, based on the detected presence of the anti-VEGF. These values were then used to provide the concentration range to test toxicity on cultured rodent and human ocular cells. The CPPs used in this study showed no apparent toxicity to any ocular cell type tested between 0.1 and 100 μg/mL.

The speed of drug penetration and delivery to the retina after application to the corneal surface of the eye is vital,¹⁸ as drugs in aqueous solution are cleared from the tear film in 15 to 30 seconds, so it was important to measure the rate of transfer of CPP + bevacizumab and CPP + ranibizumab complexes across the cornea. OCT of the rat eye over 10 minutes showed that fluorescent CPP complexes were

observed in the anterior chamber by 6 minutes. ELISA at later time points showed that levels of bevacizumab delivered by a CPP complex to retinal tissue increased over the first hour, to reach a maximum of 1 μg , representing 0.2% of the topically applied payload. Retinal levels decreased over the following 24 hours as the drug was cleared from the tissue, although the drug was still detectable in retinal tissues at very low levels after 24 hours. These results demonstrate the ability of CPP to form complexes with humanized antibody drugs and aid delivery across tissue barriers to access posterior segment target tissues in the physiologically relevant $\mu\text{g}/\text{mL}$ concentration range indicated in literature data.^{17,18} These studies were carried out in rodent eyes in which the ocular volume and delivery path length do not allow comparisons with the human eye. For example, the average thickness of the human cornea measures $535 \pm 20 \mu\text{m}$ in the center compared with $118 \pm 8 \mu\text{m}$ of the central mouse cornea.⁴⁰ Therefore, ex vivo studies were carried out in porcine eyes that have a corneal thickness of $666 \pm 123 \mu\text{m}$, making them more comparable to a human eye.⁴¹ Similar titers of antibody were delivered to the porcine posterior segment, suggesting relevance of the delivery strategy to the human eye.

The in vivo rat and ex vivo porcine observations prompt two conclusions. First, that, after topical delivery complexed to CPPs, ranibizumab and bevacizumab can access retinal tissues from the vitreous in a similar manner to that after direct ivit injection. Second, a dosing regimen that is comparable to current clinical practice is relevant to this delivery route. The current "gold standard" dosing regimen in patients is monthly injections of 300 to 500 $\mu\text{g}/\text{eye}$ ranibizumab or 100 to 300 $\mu\text{g}/\text{eye}$ bevacizumab. Preclinical studies have shown that 0.5 days after a 500 $\mu\text{g}/\text{eye}$ injection, detectable levels in the vitreous are approximately 200 $\mu\text{g}/\text{mL}$.⁴² Ranibizumab has a relatively short half-life in the vitreous of 4 days, with no detectable levels seen in preclinical trials 10 days after a single ivit injection.³⁴ Our rat study also showed that the drug cleared from the vitreous over 24 hours, allowing inferences to be made for human vitreal clearance patterns.³⁶ Clinical trials have demonstrated that, after ivit injection of 1500 $\mu\text{g}/\text{eye}$ of bevacizumab, clearance from the aqueous humor leaves 33 $\mu\text{g}/\text{mL}$ of drug at 1 day postinjection, dropping to less than 10 $\mu\text{g}/\text{mL}$ by day 18.⁴³ Human intravitreal concentrations of bevacizumab have been shown at 166 $\mu\text{g}/\text{mL}$ at 2 days postinjection and 0.5 $\mu\text{g}/\text{mL}$ at 4 weeks postinjection.⁴⁴ This indicates a target delivery level to the human retina of between 1 and 200 $\mu\text{g}/\text{eye}$ over 4 weeks. Therefore, in the porcine study reported here, the CPP + anti-VEGF ratio was optimized to effect drug delivery in this therapeutic range. The delivery of 10 to 20 $\mu\text{g}/\text{mL}$ to the posterior segment achieved in the ex vivo porcine study is within the established therapeutic range for humans (10–200 $\mu\text{g}/\text{mL}$). Although low levels of IgG were detected in the control groups, this was observed due to low levels of cross reactivity of the antibody with porcine IgG, already observed by Davis et al.⁴⁵ The topical CPP-mediated drug delivery showed drug clearance over 24 hours, with most of the anti-VEGF cleared from the ocular tissues by 4 hours. This indicates the potential for twice/thrice daily eye drops to give a repeated, sustained dose that would maintain therapeutic levels of drug in the eye for sustained periods. Future studies will determine systemic levels of the delivered anti-VEGF reflecting systemic clearance of the drug from the eye.

Once the dosing regimen and therapeutic levels achievable were determined, the CPP + anti-VEGF eye drop was tested in an established murine model of CNV to determine bioefficacy of the drug delivered using this route. It should be noted that the absence of a defined macula in mice and the laser trauma model used does not accurately mimic the complexity of the human pathology. This model is effectively a wound-healing

reaction that follows an insult at the level of Bruch's membrane and relies heavily on inflammation. In contrast in AMD, genetic susceptibility plays a major role in disease progression; hence, why steroids can be used for treatment in the mouse model but are ineffective in humans.⁴⁶ However, the mouse laser model does allow assessment of the effects of anti-VEGF on neovascularization, an important component of AMD pathophysiology.

RPE/choroid flatmount immunohistochemistry of collagen IV and isolectin B4 (as markers of neovascularization and endothelial cells, respectively, that revealed the lesion area) supported the conclusions derived from in vivo imaging of fluorescein leakage from vessels. Animals that received daily dexamethasone gavage, a single ivit anti-VEGF injection, or twice-daily eye drops for 10 days containing CPP + anti-VEGF complexes all had significantly smaller areas of collagen and isolectin B4 staining, indicative of smaller CNV lesions when compared with the three negative control groups of PBS, CPP-alone, and anti-VEGF-alone eye drops. These results obtained with eye drop delivery of CPP-anti-VEGF accord well with the results of other published studies using the CNV model to demonstrate the efficacy of a range of anti-VEGF drugs that significantly reduce the area of choroidal neovascularization.^{47–50}

In summary, these data indicate the utility of a novel noninvasive eye drop delivery mechanism for nAMD drugs. The CPP-drug eye drops have potential to significantly impact the treatment of nAMD by revolutionizing drug-delivery options. Efficacious self-administered drug application by eye drop would lead to a significant reduction in adverse outcomes and health care costs compared with current treatments. The CPP + drug complex also has potential application to other chronic ocular diseases that require drug delivery to the posterior chamber of the eye.

CONCLUSIONS

We have demonstrated a novel platform eye drop technology for ocular drug delivery that is broadly applicable because it does not require chemical conjugation of the drug chaperone. Specifically, we have shown that CPPs have high penetrating capabilities for biological barriers in the eye with low toxicity and can deliver clinically relevant concentrations of anti-VEGF drugs, such as ranibizumab and bevacizumab, to the posterior segment of the eye. In particular, these CPPs have the capacity to noninvasively deliver therapeutics in bioactive form to anterior and posterior ocular segments to give outcomes comparable to intravitreally injected drugs. If the results were translated to human eyes, it would allow the topical delivery of a wide range of ocular drugs that currently can be delivered only by ivit or subconjunctival injections. This would reduce treatment costs, time in clinic, and harmful side effects, while allowing patient self-administration, so that new drug-delivery regimens can be better tolerated.

Acknowledgments

Supported by an ARVO fellowship. In vitro testing of the drug-delivery peptides was funded by the National Institute of Health Research, Surgical Reconstruction and Microbiology Research Centre, Birmingham. Some of the experiments were performed by Neuregenix, Ltd., Birmingham, UK, that had no commercial interest in the study outcomes.

Disclosure: F. de Cogan, None; L.J. Hill, None; A. Lynch, None; P.J. Morgan-Warren, None; J. Lechner, None; M.R. Berwick, None; A.F.A. Peacock, None; M. Chen, None; R.A.H. Scott, None; H. Xu, None; A. Logan, None

References

- Rosenfield PJ, Brown DM, Heier JS, et al. Ranibizumab for neovascular age-related macular degeneration. *N Engl J Med*. 2006;355:1419-1431.
- Heier JS, Brown DM, Chong V, et al. VIEW 1 and VIEW 2 study groups, intravitreal aflibercept (VEGF trap-eye) in wet age-related macular degeneration. *Ophthalmology*. 2012;119:2537-2548.
- Bhavsar AR, Googe JM Jr, Stockdale CR, et al. Diabetic retinopathy clinical research network, risk of endophthalmitis after intravitreal drug injection when topical antibiotics are not required: the diabetic retinopathy clinical research network laser-ranibizumab-triamcinolone clinical trials. *Arch Ophthalmol*. 2009;127:1581-1583.
- Ghasemi Falavarjani K, Nguyen QD. Adverse events and complications associated with intravitreal injection of anti-VEGF agents: a review of literature. *Eye*. 2013;27:787-794.
- Elman MJ, Aiello LP, Beck RW, et al.; Diabetic Retinopathy Clinical Research Network. Randomized trial evaluating ranibizumab plus prompt or deferred laser or triamcinolone plus prompt laser for diabetic macular oedema. *Ophthalmology*. 2010;117:1064-1077.
- Brown DM, Campochiaro PA, Singh RP, et al. Ranibizumab for macular edema following central retinal vein occlusion. Six-month primary end point results of a phase III study. *Ophthalmology*. 2010;117:1124-1133.
- Green M, Loewenstein PM. Autonomous functional domains of chemically synthesized human immunodeficiency virus tat trans-activator protein. *Cell*. 1988;55:1179-1188.
- Frankel AD, Pabo CO. Cellular uptake of the tat protein from human immunodeficiency virus. *Cell*. 1988;23:1189-1193.
- Leifert JA, Whitton JL. Translocatory proteins and protein transduction domains: a critical analysis of their biological effects and the underlying mechanisms. *Mol Ther*. 2003;8:13-20.
- Vives EB, Bernard PL. A truncated HIV-1 tat protein basic domain rapidly translocates through the plasma membrane and accumulates in the cell nucleus. *J Biol Chem*. 1997;272:16010-16017.
- Derossi D. Cell internalization of the third helix of the antenapedia homeodomain is receptor-independent. *J Biol Chem*. 1996;271:18188-18193.
- Suzuki T. Possible existence of common internalization mechanisms among arginine-rich peptides. *J Biol Chem*. 2002;277:2437-2443.
- Fuchs SM, Raines RT. Pathway for polyarginine entry into mammalian cells. *Biochemistry*. 2004;43:2438-2444.
- Johnson LN, Cashman SM, Kumar-Singh R. Cell-penetrating peptide for enhanced delivery of nucleic acids and drugs to ocular tissues including retina and cornea. *Mol Ther*. 2008;16:107-114.
- Prausnitz MR, Noonan JS. Permeability of cornea, sclera, and conjunctiva: a literature analysis for drug delivery to the eye. *J Pharm Sci*. 2000;87:1479-1488.
- Hughes PM, Olejnik O, Chang-Lin J-E, Wilson CG. Topical and systemic drug delivery to the posterior segments. *Adv Drug Del Rev*. 2005;14:2010-2032.
- Urtti A. Challenges and obstacles of ocular pharmacokinetics and drug delivery. *Adv Drug Del Rev*. 2006;58:1131-11135.
- Gaudana R, Ananthula HK, Parenky A, Mitra AK. Ocular drug delivery. *AAPS J*. 2010;12:348-360.
- Jiirvinen K, Jarvinen, Urtti A. Ocular absorption following topical delivery. *Adv Drug Del Rev*. 1995;16:3-9.
- Januleviciene I, Siaudvytyte L, Barsaukaite R. Ophthalmic drug delivery in glaucoma—a review. *Pharmaceutics*. 2012;4:243-251.
- Avery RL, Pieramici DJ, Rabena MD, Castellarin AA, Nasir MA, Giust MJ. Intravitreal bevacizumab (Avastin) for neovascular age-related macular degeneration. *Ophthalmology*. 2006;113:363-372.
- Chong NV, Adewoyin T. Intravitreal injection: balancing the risks. *Eye (Lond)*. 2007;21:313-316.
- Kamei N, Morishita M, Ehara J, Takayama K. Permeation characteristics of oligoarginine through intestinal epithelium and its usefulness for intestinal peptide drug delivery. *J Con Rel*. 2008;131:94-99.
- Rothbad JB, Garlington S, Lin Q, et al. Conjugation of arginine oligomers to cyclosporin A facilitates topical delivery and inhibition of inflammation. *Nat Med*. 2000;6:1253-1257.
- Coin I, Beyermann M, Bienert M. Monitoring solid phase peptide synthesis. *Nat Protoc*. 2007;2:3247-3256.
- Berwick MR, Lewis DJ, Jones AW, et al. De novo design of Ln(III) coiled coils for imaging applications. *J Am Chem Soc*. 2014;136:1166-1169.
- Morgan-Warren PJ, O'Neill J, de Cogan F, et al. siRNA mediated knockdown of the mTOR inhibitor RTP801 promotes retinal ganglion cell survival and axon elongation by direct and indirect mechanisms. *Invest Ophthalmol Vis Sci*. 2016;57:429-443.
- Dunn KC, Aotaki-Keen AE, Putkey FR, Hjelemeland LM. ARPE-19, a human retinal pigment epithelial cell line with differentiated properties. *Exp Eye Res*. 1996;62:155-170.
- Ahmed SA, Gogal RM Jr, Walsh JE. A new rapid and simple non-radioactive assay to monitor and determine the proliferation of lymphocytes: an alternative to [³H]thymidine incorporation assay. *J Immunol Methods*. 1994;170:211-224.
- Hollanders K, Van Bergen T, Kindt N, et al. The effect of AMA0428, a novel and potent ROCK inhibitor, in a model of neovascular age-related macular degeneration. *Invest Ophthalmol Vis Sci*. 2015;56:1335-1348.
- Nishijima K, Ng YS, Zhong L, et al. Vascular endothelial growth factor-A is a survival factor for retinal neurons and a critical neuroprotectant during the adaptive response to ischemic injury. *Am J Pathol*. 2007;1:53-67.
- Nakao S, Arima M, Ishikawa K, et al. Intravitreal anti-VEGF therapy blocks inflammatory cell infiltration and re-entry into the circulation in retinal angiogenesis. *Invest Ophthalmol Vis Sci*. 2012;53:4323-4328.
- Hombrebueno JR, Ali IHA, Xu H, Chen M. Sustained intraocular VEGF neutralization results in retinal neurodegradation in the Ins2Akita diabetic mouse. *Sci Rep*. 2015;5:18316.
- Sennino B, Ishiguro-Oonuma T, Wei Y, et al. Suppression of tumour invasion and metastasis by concurrent inhibition of c-Met and VEGF signalling in pancreatic neuroendocrine tumours. *Cancer Discov*. 2012;2:271-290.
- Shah P, Desai P, Channer D, Singh M. Enhanced skin permeation using polyarginine modified nanostructures lipid carriers. *J Con Rel*. 2012;161:735-745.
- Johnson LN, Cashman SM, Read SP, Kumar-Singh R. Cell-penetrating peptide POD mediates delivery of recombinant proteins to retina, cornea and skin. *Vision Res*. 2010;50:686-697.
- Jones SW, Christison R, Bundell K, et al. Characterisation of cell-penetrating peptide-mediated peptide delivery. *Br J Pharmacol*. 2005;145:1093-1102.
- Maiolo JR, Ferrer M, Ottinger EA. Effects of cargo molecules on the cellular uptake of arginine-rich cell-penetrating peptides. *Biochim Biophys Acta*. 2005;1712:161-172.
- Liu C, Tai L, Zhang W, Wei G, Pan W, Penetratin, Lu W. a potentially powerful absorption enhancer for noninvasive intraocular drug delivery. *Mol Pharm*. 2014;11:1218-1227.

40. Zhang H, Wang L, Xie Y, et al. The measurement of corneal thickness from centre to limbus in vivo in C57BL/6 and BALB/c mice using two-photon imaging. *Exp Eye Res.* 2013;115:255-262.
41. Faber C, Scherfig E, Prause JU, Sorenson KE. Corneal thickness in pigs measured by ultrasound pachymetry in vivo. *Scand J Lab Anim Sci.* 2008;35:39-45.
42. Gaudreault J, Fei D, Rusit J, Suboc P, Shiu V. Preclinical pharmacokinetics of ranibizumab (rhuFabV2) after a single intravitreal administration. *Retina.* 2005;46:726-733.
43. Krohne TU, Eter N, Holz FG, Meyer CH. Intraocular pharmacokinetics of bevacizumab after a single intravitreal injection in humans. *Am J Ophthalmol.* 2008;146:508-512.
44. Beer PM, Wong SJ, Hammad AM, Falk NS, O'Malley MR, Khan S. Vitreous levels of unbound bevacizumab and unbound vascular endothelial growth factor in two patients. *Retina.* 2006;26:871-876.
45. Davis BM, Normando EM, Guo L, et al. Topical delivery of avastin to the posterior segment of the eye in vivo using annexin A5-associated liposomes. *Small.* 2014;10:1575-1584.
46. Lambert V, Lecomte J, Hansen S, et al. Laser-induced choroidal neovascularization model to study age-related macular degeneration in mice. *Nat Protoc.* 2013;8:2197-2211.
47. Lavalette S, Raoul W, Houssier M, et al. Intereukin-1 β inhibition prevents choroidal neovascularization and does not exacerbate photoreceptor degradation. *Am J Pathol.* 2011;178:2416-2423.
48. Tomida D, Nishiguchi KM, Katkaoka K, et al. Suppression of choroidal neovascularization and quantitative and qualitative inhibition of VEGF and CCL2 by heparin. *Invest Ophthalmol Vis Sci.* 2011;52:3193-3199.
49. Mori K, Duh E, Gehlbach P, et al. Pigment epithelium-derived factor inhibits retinal and choroidal neovascularization. *J Cell Physiol.* 2001;188:253-263.
50. Apte RS, Richter J, Herndon J, Ferguson TA. Macrophages inhibit neovascularization in a murine model of age-related macular degeneration. *PLoS Med.* 2006;3:1371-1378.